Continuum Robot Arms Inspired by Cephalopods

Ian D. Walker[a], Darren M. Dawson[a], Tamar Flash[b], Frank W. Grasso[c], Roger T. Hanlon[d], Binyamin Hochner[e], William M. Kier*[f], Christopher C. Pagano[g], Christopher D. Rahn[h], Qiming M. Zhang[i]

[a]Dept. of Electrical/Computer Engineering, Clemson Univ., Clemson, SC 29634
[b]Dept. of Computer Science & Applied Mathematics, Weizmann Inst. of Science, Rehovot, Israel
[c]Dept. of Psychology, Brooklyn College, City Univ. of New York, Brooklyn, NY 11210
[d]Marine Resources Center, Marine Biological Laboratory, Woods Hole, MA 02543
[e]Dept. of Neurobiology, Hebrew University, Jerusalem 91904, Israel
[f]Dept. of Biology, University of North Carolina at Chapel Hill, Chapel Hill, NC 27599
[g]Dept. of Psychology, Clemson University, Clemson, SC 28634
[h]Dept. of Mechanical Engineering, Penn. State Univ., University Park, PA 16802
[i]Dept. of Elect. Engineering/Mat. Sci. & Engineering, Penn. State Univ., University Park, PA 16802

ABSTRACT

In this paper, we describe our recent results in the development of a new class of soft, continuous backbone ("continuum") robot manipulators. Our work is strongly motivated by the dexterous appendages found in cephalopods, particularly the arms and suckers of octopus, and the arms and tentacles of squid. Our ongoing investigation of these animals reveals interesting and unexpected functional aspects of their structure and behavior. The arrangement and dynamic operation of muscles and connective tissue observed in the arms of a variety of octopus species motivate the underlying design approach for our soft manipulators. These artificial manipulators feature biomimetic actuators, including artificial muscles based on both electro-active polymers (EAP) and pneumatic (McKibben) muscles. They feature a "clean" continuous backbone design, redundant degrees of freedom, and exhibit significant compliance that provides novel operational capacities during environmental interaction and object manipulation. The unusual compliance and redundant degrees of freedom provide strong potential for application to delicate tasks in cluttered and/or unstructured environments. Our aim is to endow these compliant robotic mechanisms with the diverse and dexterous grasping behavior observed in octopuses. To this end, we are conducting fundamental research into the manipulation tactics, sensory biology, and neural control of octopuses. This work in turn leads to novel approaches to motion planning and operator interfaces for the robots. The paper describes the above efforts, along with the results of our development of a series of continuum tentacle-like robots, demonstrating the unique abilities of biologically-inspired design.

Keywords: Robot manipulator, biologically inspired, continuum, octopus, muscle, muscular hydrostat

1. INTRODUCTION

Most robot manipulators feature a structure inspired by that of the human arm, in the sense of being based on a serial arrangement of rigid links, connected by a relatively small (six or fewer) degrees of freedom. In this way, traditional robot manipulators are essentially "vertebrate" structures. However, traditional robots – like humans – encounter difficulties operating in highly congested environments, or in manipulating objects with parts of their arm other than their specialized end effector. These problems have been effectively addressed in nature by structures such as elephant trunks, mammal and lizard tongues, and octopus arms. These highly successful muscular structures feature significant compliance and adaptability. This paper describes our recent efforts in creating continuous backbone ("continuum") robot arms inspired by cephalopod limbs, including squid arms and tentacles, and in particular octopus arms.

There have been numerous prior attempts to create robotic "trunks and tentacles". Most of these efforts, some directly inspired by biology, have resulted in prototype hardware that has not been deployed beyond the laboratory. The reasons for this have varied, but mostly have arisen from problems in coordination/control (difficulty in coordinating the many inputs to accomplish useful tasks), and in sensing (difficulty in sensing and interpreting the surrounding environment and its interactions with the robot). We believe that the present level of scientific understanding and the current state of

technology are at a level sufficient to enable the practical solution of these two key problems. Our interdisciplinary team is conducting a coordinated program of basic and applied research aimed at incorporating new understanding of cephalopod biology in a novel and practical series of robots. Efforts range from fundamental research in cephalopod biology to applied development of robot hardware. The various key components of this effort, along with a summary of results thus far, are presented in the following sections.

2. OCTOPUS ARM STRUCTURE AND MECHANICS

The arms of octopuses, and indeed those of most cephalopods (octopus, squid, cuttlefish, chambered nautilus), consist of a tightly packed three-dimensional array of muscle fibers. As such they lack the rigid skeletal elements that characterize skeletal support in many animals such as arthropods (insects, spiders, crabs) and vertebrates. The arms of octopuses also lack the fluid-filled cavities that provide a type of skeletal support termed a "hydrostatic skeleton"[1] that is common in many invertebrate animals. The musculature of the arms of octopus not only generates the forces required for movement, deformation and changes in stiffness, it also provides the required skeletal support. This type of skeletal support system is termed a "muscular hydrostat" and is also observed in the tongues of mammals and lizards, in other portions of the bodies of cephalopods and other mollusks, and in the trunk of the elephant.[2,3]

The morphology of the muscle and connective tissues of the arms of three species of octopuses, *Octopus briareus* (elongated arms), *Octopus bimaculoides* (intermediate length arms), and *Octopus digueti* (short arms) was examined. Although the arm proportions vary in the three species, the arrangement of muscle and connective tissues was observed to be remarkably similar. A histological section taken transversely through the arm (i.e., perpendicular to the long axis) of *Octopus bimaculoides* is shown in Figure 1. The central axis of the arm is occupied by the axial nerve cord (AN), which includes both nerve cell bodies and axons (see section 4). Surrounding the axial nerve cord is a tightly packed mass of muscle and connective tissue with three major groups of muscles: transverse, longitudinal, and oblique. Muscle fibers in the transverse muscle (TM) mass are oriented in planes perpendicular to the long axis of the arm and extend to insert on connective tissue (CT) layers on the oral (side equipped with suckers, see section 6) and aboral sides, and transversely on connective tissues surrounding the oblique muscles (description follows). The transverse muscle fibers interdigitate with longitudinal muscle (LM) fibers, oriented parallel to the long axis of the arm and surrounding the central core of transverse muscle. Three pairs of oblique muscles are observed: external (EO), medial (MO) and internal (IO) oblique muscles. The external and medial oblique muscles originate and insert on the oral and aboral connective tissue layers. The connective tissue sheets consist of a crossed-fiber array, i.e., their fibers are oriented obliquely to the long axis of the arm in a highly ordered array of both right- and left-handed helixes oriented at an angle of 50-60º to the long axis. The external and medial oblique muscles are also oriented at a similar angle to the long axis of the arm and thus form a composite helical array of muscle and connective tissue fibers oriented as both a right- and a left-handed helix. The internal oblique muscles appear to have their origin and insertion on connective tissues surrounding the transverse muscle. The internal oblique muscles appear to be oriented at a smaller angle to the long axis of the arm, ranging from 40-50º.

Figure 1: Transverse histological section of arm of *Octopus bimaculoides*. See text for details.

How does this arrangement of muscle and connective tissues provide for support and movement of the arms? Because the arms lack gas-filled spaces, and because of the high bulk modulus of muscle and other tissues, the arms cannot undergo significant change in volume. Thus, if the shortening of one group of muscles decreases one dimension of the arm, some other dimension must increase. Based on this simple principle, the role of the various muscle groups in arm support and movement can be hypothesized. Elongation of a portion of the arm can be created by contraction of the transverse muscles, because their orientation will decrease the cross-sectional area. Shortening of the arm results from

contraction of the longitudinal muscles; the cross-sectional area will increase, re-elongating the transverse muscles. Thus, the transverse and longitudinal muscles can be considered to be antagonistic muscles. Torsion (twisting around the long axis) of the arm will result from contraction of the external and medial oblique muscles. The direction of torsion depends on the handedness of the oblique muscle array; both right- and left-handed arrays are present and thus torsion in either direction is possible. The role of the internal oblique muscles in arm movements is unclear. Bending of the arm can be caused by contraction of longitudinal muscles on one side of the arm and requires that the transverse muscle contract simultaneously in order to resist the longitudinal compressional forces caused by contraction of the longitudinal muscles. The flexural stiffness of the arm can be increased by co-contraction of the longitudinal and transverse muscles. An important characteristic of this biomechanical system is the fact that the movements and deformations outlined above can be highly localized. Thus, there is the potential to combine these deformations on a single arm to create a more complex array of movements, as described in the following section.

3. OCTOPUS ARM MOVEMENTS

The aim of the research on arm movements is to determine the most basic set of arm movements that a single octopus arm is capable of, and to relate these movements to the muscles of the arm described above and to their neural control described below. A comparative approach has been taken: 18 species of octopus have been videotaped performing a wide range of arm movements, often in response to a test set of differently sized and shaped objects. These species include short-, medium- and long-armed octopuses. Over 200 video sequences (recorded in the laboratory or in nature) were analyzed frame-by-frame. Locomotory arm movements have been excluded.

We determined that *all arm movements are the result of the need to bring the "oral surface of the arm" (i.e., the suckers) to bear on a task.* The oral surface of the arm appears to be the sole "work surface" of the arm. A striking finding was the dexterity and wide range of movement of individual arms in all 18 species. We detected no obvious gross motor differences among short-, medium- or long-armed species. As described above, each arm or portion of the arm is capable of elongation, shortening, stiffening, bending and torsion. Each of these components can occur alone, but most commonly they occur in synchronized combinations that result in three basic movements.

REACH. This is defined operationally as an increase in the distance between the proximal and distal portions of the arm. We can distinguish an uncurling reach, a straight elongating reach, a rapid strike, and a slow forceful push of an object.

PULL. This is defined as a decrease in the distance between the proximal and distal portions of the arm. We can distinguish a curling pull, muscular arm shortening, a bending pull, and a torsional retraction.

SEARCH/GROPE. This is defined operationally as arm movements in which there is no substantial change in distance between the proximal and distal portions of the arm. We can distinguish whole-arm bends (no torsion), localized bending (often associated with torsion), and arm-tip wraps.

Many functional behaviors are accomplished with these three basic arm movements. The suckers provide strong adhesion using suction, they are heavily innervated, and they have sensory capabilities that include touch and taste discrimination. Thus, each arm works in seemingly perfect coordination with approximately 200 suckers, and also with the other 7 arms.

One particularly noteworthy – and counterintuitive - arm behavior was observed in these species. When an octopus reaches out and grasps an object, it does not grasp with the tip of the distal arm. The arm makes contact at a point about 1 cm from the tip, attaches with several suckers, then quickly wraps the tapered tip around the object in several directions as though sensing it.

The next step will be to describe the behaviors associated with each type of arm movement, and to determine the most common combinations of reach, pull and search/grope that produce these behaviors. Eventually, we wish to explain arm behaviors not only in terms of "reach, pull and search/grope," but to describe the combination of localized elongation, shortening, stiffening, bending and torsion that is responsible for overall arm movements. This understanding will be crucial for understanding the neural control of arm movements, described in the following section.

4. NEURAL CONTROL OF THE OCTOPUS ARM

4.1 Behavioral, physiological and kinematic studies

Behavioral and physiological approaches were used to investigate how the octopus generates and controls its whole limb movements in reaching and pulling. We found that the octopus has evolved highly efficient control strategies, probably driven by the complex interaction between the motor system (8 highly flexible arms) and the relatively small central brain (~5 X 10^7 neurons). In particular, the octopus has evolved two unique control strategies to cope with these complexities. The first consists of using highly stereotypical movements that reduce the infinitely large number of degrees of freedom of the arms to only a few controlled variables. The second is reflected in the unique division of labor between the central and the peripheral nervous systems, with special reliance on the highly evolved peripheral nervous system of the arms for both control and execution of the spatio-temporal details of activation commands.

Reaching movements such as the uncurling reach described above start with the formation of a bend somewhere along the arm. This bend is then propagated towards the tip of the arm with the proximal portion of the arm remaining stiff and straight, the bend propagation showing an invariant tangential velocity profile (when normalized for movement duration and maximal velocity).[4] Because the extension is restricted to a linear plane, the extension movement is constrained to only three degrees of freedom - two for direction and one for scaling of the speed of bend propagation. Arm extensions with similar kinematics to those seen in freely behaving animals can be induced by electrically stimulating arms that are disconnected from the brain.[5] The motor program for reaching must therefore be embedded within the neuromuscular system of the arm itself, including the axial nerve cord. We have also demonstrated that this program is based on a strong feed-forward mechanism.[6] All these findings suggest that the control of arm extension is enormously simplified by restricting the number of controlled variables and by the brain being required to command and scale only a fixed-action program located in the peripheral neuromuscular system.

A different strategy has evolved for the generation of fetching movements such as the bending pull described in section 3 above.[7] Octopuses can reach and grasp a target anywhere along the arm using the suckers, which are distributed along the entire length of the arm. However, when pulling the grasped object to the mouth, a precise point-to-point reaching task must be executed - the end-effector (the site on the arm grasping the object) must reach a specific target (the mouth) – similar to reaching tasks performed by articulated arms (Fig. 2). The movement starts with the creation of an articulated-like structure composed of three localized bends that behave like joints in rigid skeletal structures. In striking similarity to the geometry of vertebrate arms, the proximal (L_1) and the medial segments (L_2) are nearly identical in length. Uniquely to the octopus, however, this articulated-like structure is adjusted for each pulling movement according to the position along the arm the object was grasped. Following the formation of the localized bends, the distal bend is accurately brought to the base of the arm mainly by rotating the segments around the medial joint. Finally, rotations of the distal segment (L_3) bring the object to the mouth. Kinematic analysis shows that the movement is restricted to a single linear plane; once again the control of the movement involves three degrees of freedom - one for each joint. The analysis also shows that octopuses seem to control the rest of the pulling movement in joint space, thus avoiding the complexities of the inverse kinematics transformation in hyper-redundant structures. Taken together, these motor organization and control mechanisms greatly simplify the problems associated with the generation of efficient point-to-point movements using flexible arms.

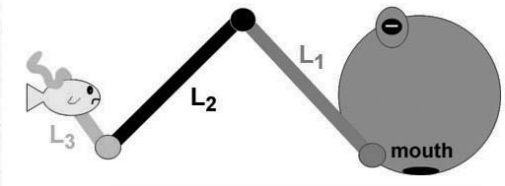

Figure 2: Octopus bending pull (fetching) movements involve a *quasi*-articulated structure based on three joints (see text).

4.2 Modeling approaches

Given that the octopus arm lacks a rigid skeletal support and consists almost entirely of muscle and connective tissues, it requires special control systems. To investigate the nature of these control schemes, a 2D dynamic model of the octopus arm was developed[8] that explores possible strategies of movement control in this muscular hydrostat. The octopus arm was modeled as a multi-segment structure (Fig. 3), each segment containing longitudinal and transverse muscles and maintaining a constant volume. The input to the model is the degree of activation of each of its muscles. The model includes the external forces of gravity, buoyancy and water drag forces whose magnitudes were experimentally evaluated. The model also includes the internal forces generated by the arm muscles and the forces responsible for maintaining a constant volume. The equations of motion for the multi-segment arm were then derived.

Assuming that the input to the model consisted of the degree and time-dependency of activation of all the muscles, the mechanisms and characteristics of bend propagation that could result in arm extension movements with similar characteristics to those experimentally observed were investigated. Based on extensive computer simulations of arm extension movements we found that: (1) a simple command producing a wave of stiffening due to similar activation levels to all the three muscle groups, moving at a constant velocity, is sufficient to replicate the natural reaching movements with similar kinematic features; (2) the biomechanical mechanism that produces the reaching movement is a stiffening wave of muscle contraction that pushes a bend forward along the arm; (3) given that the perpendicular drag coefficient was found to be ~50 times larger than the tangential drag coefficient, our analysis also showed that the reaching movements performed by the octopus minimize the influence of the perpendicular drag forces.

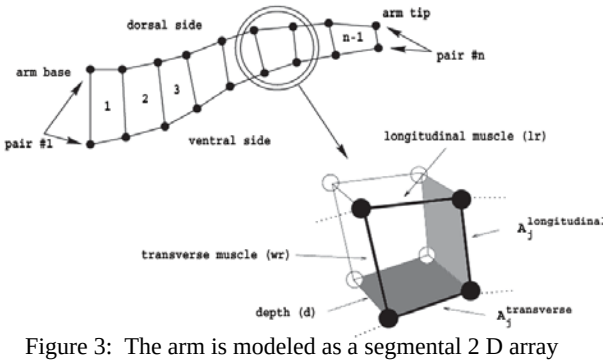

Figure 3: The arm is modeled as a segmental 2 D array of point-masses and springs (see text).

The dynamic model of the octopus arm[8] was further used to investigate the neural strategies that may be employed by the octopus nervous system to control arm reaching movements.[9] The control of only two parameters was found to be sufficient to fully specify the extension movement: the *amplitude* of the activation signal (leading to the generation of muscle forces of different magnitudes) and the *activation traveling time* (the time the activation wave takes to travel along the arm). We found that the same movement kinematics could be achieved by applying activation signals with different activation amplitudes all exceeding some minimal level. This suggests that the octopus nervous system might employ a minimal amplitude of activation to generate the minimal muscle forces required for the production of the desired kinematics. Larger amplitude signals would generate larger forces that enhance the arm's stability against perturbations without changing the movement kinematic characteristics. The robustness of this phenomenon was demonstrated by examining activation signals with either constant or bell-shaped velocity profiles. The results from the above modeling efforts suggest that the biomechanical properties of the octopus arm may allow independent control of the movement kinematics and the resistance to external perturbations occurring during the arm extension movements.

Recently, a model-based control algorithm for a hyperredundant soft manipulator was developed.[10] The model uses the above dynamic model of the octopus arm. Assuming that the arm muscles can be modeled as visco-elastic elements, the arm potential energy was minimized and based on the treatment of the arm as composed of a series of segments, the muscle activation patterns required for the arm to follow a prescribed trajectory, described by a time-varying curve were derived. The algorithm was implemented in computer simulations, and tested for various movement tasks. Recorded live octopus movements were used as an input to the algorithm, and the resulting activation patterns were computationally derived and analyzed. These were then introduced as inputs to the arm full dynamic model to test whether the activation patterns calculated using the model-based algorithms can lead to realistic arm trajectories when fed back into the full dynamic model.

4.3 Future directions

The above experimental results and models show that our approach can advance our understanding of the underlying control mechanisms in the octopus and will be implemented in control of our flexible robotic arms. Further investigations of more complex movements in three dimensions are planned.

5. ROBOT ARM DESIGN AND PERFORMANCE

Taking inspiration from the structure, mechanics, and movement of octopus arms, a highly dexterous, high-DOF soft robotic manipulator, named "OCTARM", was designed and constructed. Unlike typical laboratory robots, OCTARM has the additional strength, durability, and mobility to operate in the field. The 110 cm long manipulator is easily portable and vehicle mounted. Current robotic arms are not compliant with large or awkward objects, and lack the ability to manipulate these loads. OCTARM's conforming soft structure has the ability to grasp objects of various sizes and shapes and manipulate them in confined environments.

OCTARM moves using McKibben air muscles as actuators (Fig. 4). Common inflation pressures range from 2-9 bar. These air muscles have a large strength-to-weight ratio, allowing OCTARM to remain lightweight (18 N) but powerful. The actuators are similar in many regards to the muscles found in muscular hydrostats such as octopus arms. Actuation force depends both on the air pressure used for inflation as well as the cross-sectional area of the actuator. In total, OCTARM uses eighteen air muscles that extend when pressurized. The extension actuators all have large strains (> 40%). These large strains allow for great dexterity and arm manipulation range.

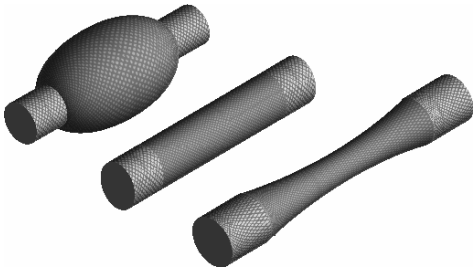

Figure 4: McKibben air muscle actuators.

Figure 5: OCTARM.

OCTARM (Fig. 5) consists of four, uniquely designed sections, each nearly 30 cm in length. Each section has two-axis bending plus extension so that OCTARM has a total of 12 DOF. There is a design trade-off between holding force (maximum applied moment) and curvature in each section. Greater moment forces can be obtained by increasing the radial distance between the central axis and the actuator location; decreasing this distance generates increased curvature. OCTARM's two proximal sections have six actuators arrayed about the central axis. Each of the distal two sections has three actuators closely packed together for the greatest curvature. This creates the tapered shape to the arm. Proximal sections of the arm are stronger than those at the distal tip, but weigh more and are not capable of achieving the same curvature. Muscles in all sections are constrained radially by connecting the muscles to each other and to the constraining outer covering. This connectivity distributes stress concentrations, allows for longitudinal motion and curvature, and prevents gaps and bulges in the flexible actuators.

Air is supplied to the actuators in each section by flexible tubing that runs inside the arm. Computer automated pressure regulators control airflow from the high-pressure tanks to OCTARM's base plates. A total of five plates separate OCTARM's segments and provide a location for mounting the muscles (Fig. 6). These plates serve a dual purpose. First, they link sections, supporting the soft actuators. Secondly, they act as manifolds for air distribution to individual actuators. Using this distribution system, actuation time is nearly instantaneous.

Figure 6: Base plate.

OCTARM is capable of high tip speeds in excess of 0.8 m/s. At low pressures (4.5 bar), OCTARM can lift a maximum vertical load of 12 kg and a transverse load of 0.5 kg. By changing the actuation pressure, OCTARM can manipulate objects of many sizes and maneuver in confined spaces, limited by the minimum radius of curvature in the last section (5 cm). When higher air pressures are available, both load capacity and radius of curvature improve significantly.

6. ARTIFICIAL SUCKER MODELLING AND DESIGN

6.1 Introduction

OCTARM will eventually be equipped with artificial suckers for use in adhesion and fine manipulation inspired by those of cephalopods. Cephalopods have a diversity of sucker mechanisms for grasping, adhering to and manipulating objects or surfaces. Many nearshore squids such as *Loligo sp.* use simple piston-like suckers that attach to prey on contact.[11] Open ocean cephalopods like the Humbolt Squid *Dosidicus sp.* possess suckers dwarfed by arrays of protruding chitinous hooks.[12] The suckers attach to the prey and then the arm or tentacle moves the food to the mouth. Octopuses put their suckers to more elaborate uses. In addition to reversibly attaching objects to the arm, single suckers can

transport objects short distances along the arm. Groups of suckers, acting in coordination, can move small objects along the arm, and/or rotate the objects in place. Our research is aimed at translating these abilities to robot suckers for use in reversible adhesion and fine manipulation on the OCTOR robot arm. For a relatively low energetic investment the octopus may, on command, generate and release approximately 2 atmospheres of negative pressure for adhesion in less than a second.[13] This is achieved through two sets of muscles arranged in a geometry that uses the bulk modulus of water to advantage. These morphological adaptations also allow the octopus to hold an object in a tenacious grasp indefinitely. Reversible grasping of this type is desirable for the OCTOR arm as it reduces the reliance of the arm on surface friction for grasping tasks.

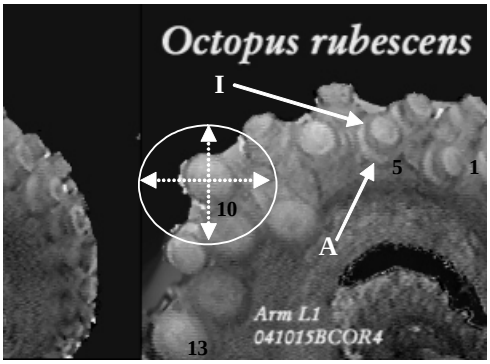

Figure 7: Flexed octopus arm with double row of 13 suckers. Infundibulum (I) and acetabulum (A) on sucker **5**. Dashed arrows & circle: radius of rotation by (sucker **10**) extrinsic muscle action.

6.2 The Sucker Operation Cycle

In the octopus sucker adhesion is produced by the coordination of muscles in two continuous structures called the acetabulum and the infundibulum (Fig. 7). These form the internal cavity of the sucker and the rim that is applied to the object being grasped, respectively. Sucker movement relative to the arm is achieved by an array of extrinsic muscles that connect the sucker to the arm.[13] We refer to the sequential activation of these muscles that produces adhesion and sucker movements for manipulation as the sucker operational cycle (SOC). In the infundibular phase of the SOC, the infundibulum extends until the entire circumference of the rim contacts a surface. The infundibulum, which is easily deformed by muscle, conforms to the surface to produce a seal that separates the fluid inside the hollow interior from that outside. With the seal formed, the acetabulum changes shape. This shape change, which involves dilation of the internal cavity, produces negative pressure inside relative to ambient. Suction, and thus adhesion, is maintained as long as the musculature of the acetabulum exerts force. With the surface firmly held the extrinsic muscles can be employed to rotate the sucker in any direction. Finally, the acetabulum relaxes and the internal pressure returns to ambient, releasing the adhesion.

6.3 Modeling sucker operation

We developed a simulator to model the sucker cycle and study its control. As in the octopus, the essential building blocks are the muscular hydrostat units (MHUs) and the connective tissues that transmit force and control deformation. The MHUs are modeled as constant volume cylinders under the action of internal muscle fibers that reduce one or more dimensions. Assemblies of MHUs are held together by a network of connective tissue fibers that are modeled as springs. (Fig. 8). As MHUs are reshaped by contraction of specific muscle fiber orientations, they push against each other and the connective network to arrive at dynamic equilibrium. The simulation is built from first principles and uses literature values for biological or artificial materials. We have validated the model at the MHU level by comparing simulation results for contraction velocity with physiological values and at the MHU assembly level by reproducing squid tentacle extension dynamics with a biologically-scaled model. We studied a virtual sucker that modeled the acetabulum with seven MHUs, the infundibulum with six units, and six extrinsic muscles. The simulator was capable of reproducing each phase (infundibular extension, acetabular shape change and extrinsic muscle mediated rotation) singly with quantitatively biological dynamics and displacements. We are currently conducting simulations to coordinate these phases and reproduce the sucker operation cycle.

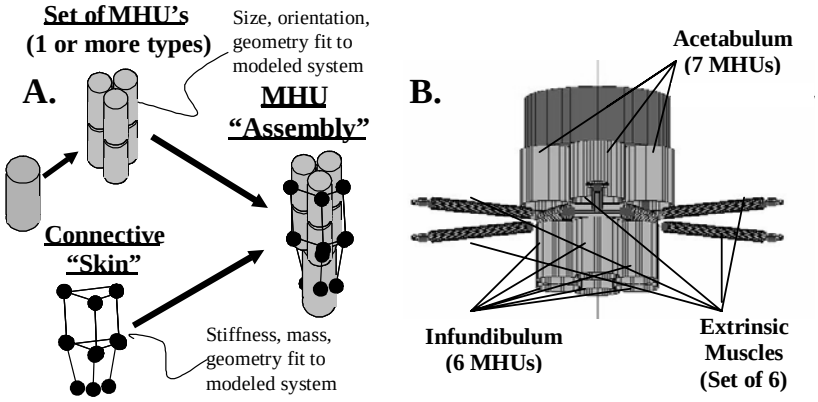

Figure 8: Model MHU systems. **A.** Assemblies of MHUs spatially constrained by connective skins. **B.** 3d rendering of the assembly for modeling octopus suckers.

6.4 Future Robot Implementation

Once the biologically constrained sucker model is validated and the control mechanisms understood, the simulator will become a virtual prototyping system. We plan to replace the parameters used to simulate the materials of the biological system with those of man-made materials. This approach has been shown to be plausible in the squid tentacle simulation studies in which we replaced the connective tissue parameters with those of rubber, and the contractile properties of the MHUs with EAP artificial muscle. Our current aim is to parallel the tentacle studies with model suckers inspired by those of octopuses. Detailed video of live octopus suckers will be used to refine and compare the sucker modeling efforts.

7. ELECTROACTIVE POLYMER ACTUATORS

Although OCTARM currently uses McKibben air muscle actuators, we are also investigating electroactive polymer (EAP) actuators for potential future use in the arm. Two types of EAP actuators are investigated: PVDF based electrostrictive polymers and dielectric elastomers (DE).[14-16] Both possess the required high elastic energy density and fast response.

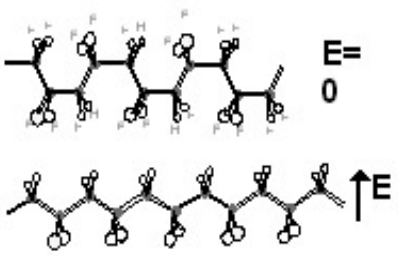

Figure 9: Schematic illustrating the strain changes between the non-polar (TGTG') and polar (all-trans) molecular conformations which can be induced by external electric field.

The actuation of PVDF-based electrostrictive polymers such as P(VDF-TrFE-CFE) terpolymers, where CFE is chlorofluoroethylene (CFE, -CH_2-CFCl), originates from the electric field induced molecular conformation change between the non-polar, which is a mixture of trans-gauche (TGTG') and T_3GT_3G' and polar conformation (all-trans conformation) forms. As schematically shown in Figure 9, a strain of larger than 10% can be achieved along the polymer chain direction accompanying the molecular conformation changes. Different from the normal ferroelectric P(VDF-TrFE) copolymer in which this conformation change does not occur reversibly, the PVDF based terpolymers which include a small amount of properly selected termonomer is a relaxor ferroelectric and the conformation changes between the polar- and non-polar conformations proceed reversibly. Consequently, large electrostriction is obtained with these terpolymers. For example, for a terpolymer of P(VDF-TrFE-CFE) 68/32/9 mol%, a thickness strain of more than 7% (Fig. 10(a)) and a transverse strain of 5% [Fig. 10(b), stretched polymer films measured along the drawing direction] can be achieved. These polymers show very high frequency response (above 100 kHz) with an elastic energy density above 0.5 J/cm^3.

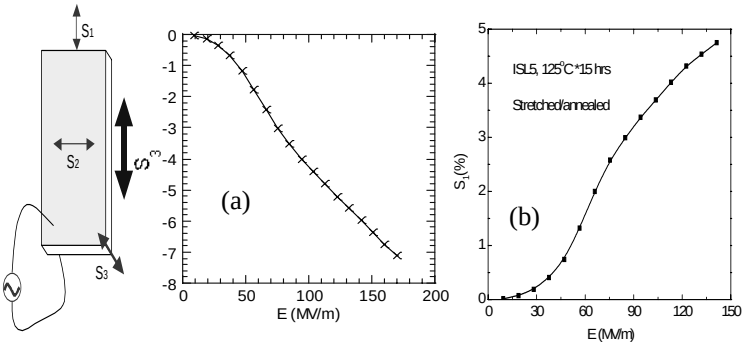

Figure 10: Thickness strain (a) and transverse strain of a uniaxially stretched P(VDF-TrFE-CFE) terpolymer.

The dielectric elastomers are actuated by the electrostatic force (Maxwell stress). In this investigation, a commercial DE (3M VHB 4905) was used, which has a thickness of 0.5 mm. In order to reduce the driving voltage (these DEs require more than 100 V/μm to achieve high strain), the material was biaxially stretched to reduce the thickness to 60 μm. To increase the load capability, the pre-stressed

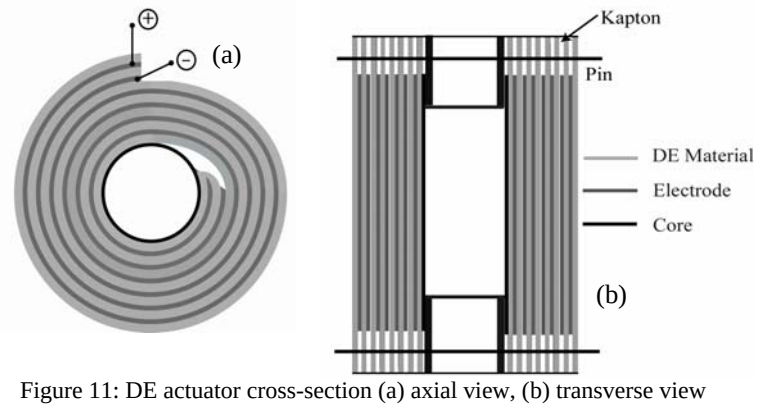

Figure 11: DE actuator cross-section (a) axial view, (b) transverse view

material was wound around a radially rigid core (an extension spring core, which is axially flexible, allowing the axial motion of the DE actuator. For the actuators fabricated here, the core radius is 4.77 mm). Figure 11 shows the DE actuator design, in which conductive carbon grease was used as the electrodes. Several actuators were tested. For example, for a DE actuator with a length of 12 cm with 15 DE layers, a maximum strain of 12.7% was obtained under a voltage of 3.64 kV. The actuator also exhibits a stiffness of 157 N/m. In addition, an axisymmetric Finite Element Method (FEM) model with electrostatic and radial bulk modulus nonlinearity predicts actuation displacement and stress. The maximum compressive radial stress occurs at the center of the innermost active layer. This layer also has the thinnest material, indicating the most likely failure point. A comparison of the model prediction and experimental results is presented in Figure 12.

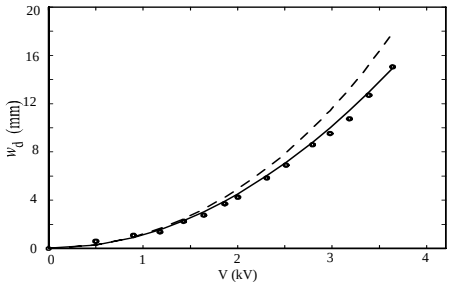

Figure 12: Displacement versus voltage for an DE actuator. Nonliear theory (- -), linear theory (--), and experiment (.)

7. CONTROL ALGORITHMS

To exploit the physical capabilities of the unique robot hardware described in the preceding sections, novel algorithms need to be developed and implemented. In particular, the inclusion of multiple and redundant degrees of freedom within the robots, and their nonintuitive (to the human operator) arrangement and function, pose significant challenges. Our approach to addressing these challenges is summarized in this and the subsequent sections.

7.1 Kinematic Modeling and Low-level Control

At the lower (kinematic) level, algorithms are needed to accurately convert between robot shapes and tasks and the actuator inputs that provide them. For this, we have adopted a modular three step approach. First, we fit a conceptual "phantom" rigid-link manipulator to the central backbone curve of the real arm. This allows us to use a modification of conventional (Denavit-Hartenberg) manipulator kinematic models to relate task space coordinates (trunk tip, trunk grasp locations) to robot shape parameters (section lengths, curvatures, and angles of curvature). In this step, the joint angles of the phantom arm are exploited to introduce the robot shape parameters. Second, we use geometric methods to find closed-form expressions relating the robot shape parameters to the length of the air muscle actuators. More details of these transformations are given in Jones and Walker.[17]

The third step in the kinematics development is to convert actuator lengths to nominal input pressures. This is currently achieved via an empirically-derived model. The nominal actuator pressures are currently fed into a simple low-level PID controller to achieve desired shapes (currently arising input via joystick input, see below and section 8 for more details). We are currently developing a more sophisticated strategy for integrated control and path/task planning. This activity is summarized in the following subsection.

Input to the robot is achieved via a joystick interface (typically we use a Wingman 3D joystick from Logitech). The joystick is interfaced to a laptop PC, and passed via a wireless link to a local PC104-based computer (on which the kinematics and control loop are running in real time). The human operator can command each lower level movement (section extension, curvature, or angle of curvature) individually, or collectively in primitives or synergies (see section 8.). The operator input can be at either position or velocity level.

7.2 Integrated Path Planning and Control

One important advantage of hyperredundant robot manipulators is the ability to do whole-arm grasping of objects. Whole arm grasping can be done by contacting the object in a snake, or tentacle-like manner, using portions of the manipulator to wrap around the object and grasp it. This capability could be used in many applications, such as search and rescue, underwater and space exploration. Roughly speaking, the whole arm grasping objective is achieved by integrating the path planner and the controller such that two tasks, *robot end-effector positioning* and *robot body self-motion positioning*, are accomplished simultaneously. The *end-effector positioning* control design forces the end-effector to follow a path around the object which in turn, forces the robot's body to wrap itself around the object to be

grasped. The *body self-motion positioning* control design "repels" the body of the manipulator away from the object while the end-effector moves around the object. This control-induced repulsion-like property removes the "slack" from the robot as it begins to move into the grasping position. When all possible slack is removed, the manipulator makes contact with the object hence completing the whole arm grasping of the object. Figure 13 demonstrates one possible posture for whole-arm grasping of a spherical object.

To facilitate the explanation for approach to whole-arm grasping, using hyperredundant robots, we first note that the novel Denavit-Hartenberg based kinematic model for an n-segment hyperredundant manipulator can be written as follows

$$\dot{x} = J(q)u$$

where q is a vector of link-space joint angles, $\dot{x}$ is the end-effector's velocity, $J(q)$ is the non-linear non-symmetric Jacobian matrix, and u is the kinematic control input.

The kinematic controller u is designed as follows, to achieve both control objectives simultaneously

$$u = J^{+}U_e + \left(I_n - J^{+}J\right)U_m$$

where J^{+} is the pseudo-inverse of the Jacobian matrix, U_e is the auxiliary *end-effector positioning* control input and U_m is the auxiliary *body self-motion positioning* control input. The auxiliary *end-effector positioning* controller is designed as follows

$$U_e = \dot{x}_d + K_s\left(x_d - x\right) \quad \text{and} \quad \dot{x}_d = \vartheta(x)$$

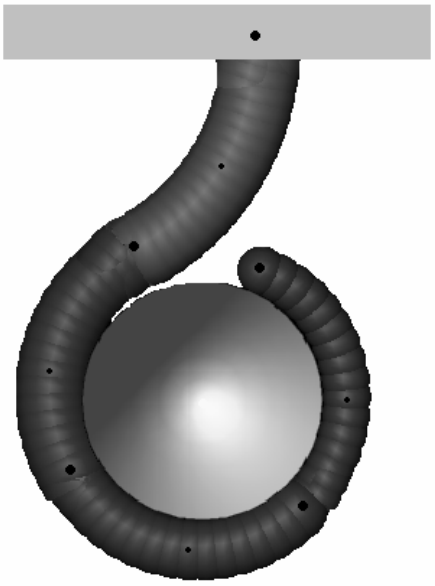

Figure 13: Hyperredundant robot manipulator demonstrating whole arm grasping.

where K_s is diagonal control gain matrix, x_d is desired position generated by the velocity field, $\vartheta(x)$ is a task-space velocity field. For the circular object as seen in Figure 13, the velocity field generates a desired trajectory that forces the end-effector to spiral inwardly towards and around the surface of the object, see [18] for details of circular velocity field. The auxiliary *body self-motion positioning* controller is designed as follows

$$U_m = -\left[\left[\frac{\partial y_a}{\partial q}\right]\left(I_n - J^{+}J\right)\right]^T y_a$$

where I_n is the standard *nxn* identity matrix, y_a is a repulsive auxiliary function that encodes the geometric information about the object's surface and how it relates to the manipulator's link positions in an effort to keep the body of the manipulator away from the object, see E. Tatlicioglu *et al.*[19] for details of a general repulsive auxiliary signal for self-motion control of a redundant robot manipulator. Interestingly, as the slack in the robot body is removed, the effects of the control term U_m are automatically reduced (i.e., the matrix related terms multiplying y_a become almost zero).

8. INPUT DEVICES FOR ROBOT CONTROL

The motion planning and control of a human-operated hyperredundant continuum robot requires that the operator be continuously aware of the current state of the robot (e.g., limb curvature and deformations, location, velocity), the dispositions of objects and surfaces in the environment (e.g., distances, inertia, compliance), and the relative positioning between the robot and objects in the environment. Manipulations require dexterous planning and control of robot dynamics via the operator interface. The challenge is to effectively interface the many degrees of freedom inherent in continuum robots with human operators. It is interesting to note that among animals featuring trunk and tentacle manipulators; there is usually a set of stereotyped behaviors, or "synergies," which combine primitive movements to produce complex motions with fewer degrees of freedom under explicit control by the higher levels of the nervous system. The same is also true of humans and complex-limbed animals in general. The problem of controlling many degrees of freedom is made tractable in natural systems by the formation of synergies - ensembles of muscle and joint

linkages that are harnessed to act in coordination.[20,21] Our design of a human interface is guided by the creation of synergies, input devices with few degrees of freedom that allow the operator to intuitively control the many degrees of freedom inherent in the robotic system.

Automobile steering is a good example of a synergy in human-factors engineering. Imagine driving a car equipped with two steering wheels, one providing input to each of the two front wheels. Such a system would inevitably result in errors involving the application of non-optimal combinations of wheel angles. The solution is to design an interface that allows many separate degrees of freedom to be operated by an interface with far fewer degrees of freedom. A synergy links parts together so they are no longer free to vary independently, eliminating configurations that would result in uncoordinated movements. System performance can be enhanced by increasing the complexity of the synergy without altering the complexity of the human interface. For a car to turn smoothly the inside wheel makes a tighter turn than the outside wheel. The steering linkage is such that the inside wheel turns more than the outside wheel, and thus the operator need not be aware of the optimal wheel angles for each given turn. Synergies also allow optimal configurations of separate degrees of freedom to change as a function of other parameters. With four-wheel steering, for example, the relation between the angles of the front wheels to the angles of the rear wheels changes as a function of vehicle speed. At low speeds, the rear wheels are turned in the opposite direction of the front wheels, at moderate speeds the rear wheels remain straight, and at high speeds the rear wheels are turned in the same direction as the front wheels. A control unit determines the appropriate angles for the rear wheels by continuously monitoring steering wheel position sensors and vehicle speed sensors. Thus the steering synergy can be expanded to four wheels without increasing the cognitive burden imposed on the operator. In biological systems, such synergies are formed and reformed in lower levels of the nervous system, such as the spinal cord or in the neuromuscular system of the octopus arm itself (see section 4 above), to create linkages among muscles that become constrained to act as single functional units.[21] The use of synergies as a principle for the design of human-operated robotic system is an example of the fruitful application of biological inspiration.

As described above, OCTARM consists of four segments, with each segment consisting of either three pneumatic muscles or six pneumatic muscles arranged in three sets of linked pairs. Twelve valves control the muscles, each regulating the pressure for one of the three muscles or muscle pairs in each segment of the robot limb. The human operator needs to control both the degree of curvature and the direction of curvature for each of the limb segments. The mapping from the twelve valves to the direction and degree of curvature for the four segments is, however, intractably complex for a human operator. Thus an optimum human interface would not consist of twelve input devices, each independently operating one of the valves. We have developed a joystick-based interface that allows the operator to input the desired direction and degree of curvature for each of the limb segments. Synergies built into the controller translate the inputs into the correct combinations of settings for the twelve valves. One example of a synergy can be seen by examining the relationship between the direction in which a limb segment is curved, the length of the segment, and the resulting maximum possible curvature of that segment. In a 2-dimensional parameter space composed of segment length and direction of curvature, there exists a line along which maximum curvature is achieved. Deviations from this line result in a dramatic reduction of curvature. Since a continuum limb relies on encircling an object in order to grasp it, a reduction of curvature often causes the limb to drop an enclosed object. Thus the operator must navigate along the line of maximum curvature to manipulate a grasped object. The curvature of the line, however, is quite complex, so the operator finds it very difficult to move a grasped object through space without dropping it. A synergy that automatically chooses the optimal trunk length for a given trunk direction or vice versa was found to be critical to the arm's ability to grasp and manipulate objects. By synergistically varying arm length with the operator's input of desired changes in limb direction, maximum curvature at any limb direction can be maintained, freeing the user to select direction without also manually selecting matching segment lengths.

9. CONCLUSIONS

The paper has summarized our initial efforts in developing continuous backbone “continuum” robot limbs inspired by the limbs of cephalopods. We have already made some interesting and unexpected discoveries regarding the structure and operation of octopus arms. The parsimony in arm structure and function found among the octopus species studied provides inspiration for developing a robotic arm that can produce a similar diversity of movement. Some of this new understanding has already been incorporated into our prototype robots. We have demonstrated the ability to coordinate the inputs of these robots to achieve useful tasks. The robots are currently undergoing field demonstrations. Our current

activities focus on the sensory needs and capabilities of both cephalopods and continuum robots and the goal of incorporating torsional movements in the robots. Results from these ongoing efforts will be reported in future publications.

ACKNOWLEDGMENTS

For work on live octopuses at the MBL, we thank P. Alatalo and J. Forsythe, and we are grateful for the efforts of interns W. McCord, A. Neway, C. Gupta, and C. Plautz. We thank S. Guarda and M. Stella for assistance with the octopus morphology investigations. This work was supported in part by DARPA under Contract N66001-C-8043 and by the Israel Science Foundation (580/02)..

REFERENCES

1. G. Chapman, "The hydrostatic skeleton in the invertebrates," *Biol. Rev. Camb. Philos. Soc.* **33**, 338-371, 1958.
2. W.M. Kier and K.K. Smith, "Tongues, tentacles and trunks: the biomechanics of movement in muscular hydrostats," *Zool. J. Linn. Soc.* **83**, 307-324, 1985.
3. K.K. Smith and W.M.Kier, "Trunks, tongues and tentacles: moving with skeletons of muscle," *Amer. Sci.* **77**, 28-35, 1989.
4. Y. Gutfreund, T. Flash, Y. Yarom, G. Fiorito, I. Segev, "Organization of octopus arm movements: a model system for Studying the Control of Flexible Arms," *J. Neurosci.* **16**, 7297-7307, 1996.
5. G. Sumbre, Y. Gutfreund, G. Fiorito, T. Flash, B. Hochner, "Control of octopus arm extension by a peripheral motor program," *Science* **293**, 1845-1848, 2001.
6. Y. Gutfreund, T. Flash, G. Fiorito, and B. Hochner, "Patterns of muscle activation involved in octopus reaching movements," *J. Neurosci.* **18**, 5976-5987, 1998.
7. G. Sumbre, G. Fiorito, T. Flash, B. Hochner, "Neurobiology: Motor control of flexible octopus arms", *Nature* **433**, 595-596, 2005.
8. Y. Yekutieli *et al.*, Submitted, 2005a.
9. Y. Yekutieli *et al.*, Submitted, 2005b.
10. I. Gendelman, M.Sc thesis, Weizmann Inst. of Science, 2005.
11. W.M. Kier, "The functonal morphology of the musculature of squid (Loliginidae) arms and tentacles, " *J. Morph.*, **172**, 179-192, 1982.
12. M. Norman, *Cephalopods. A World Guide*, ConchBooks, Hachenheim, 2000.
13. W. M. Kier and A.M. Smith, "The morphology and mechanics of octopus suckers," *Biol. Bull.*, **178**, 126-136, 1990.
14. Q.M. Zhang, C. Huang, F. Xia, J. Su., in *Electroactive Polymer (EAP) Actuators as Artificial Muscles – Reality, Potential, and Challenges, 2nd ed.* (Ed: Y. Bar-Cohen), SPIE, Bellingham, WA, 2004.
15. Q. M. Zhang, V. Bharti, X. Zhao, **"**Giant electrostriction and relaxor ferroelectric behavior in electron-irradiated poly(vinylidene fluoride-trifluoroethylene) copolymer," *Science* **280,** 2101-2104, 1998.
16. R. Pelrine, R. Kornbluh, Q. Pei, and J. Joseph, "High-speed electrically actuated elastomers with strain greaqter than 100%," *Science*, **287,** 836-839, 2000.
17. B. Jones and I.D. Walker, "A new approach to Jacobian formulation for a class of multi-section continuum robots," *Proceedings of the IEEE International Conference on Robotics and Automation*, Barcelona, Spain, 2005.
18. M. McIntyre, W. Dixon, D. Dawson, and B. Xian, "Adaptive tracking control of on-line path planners: velocity fields and navigation functions," *Proceedings of the American Controls Conference*, Portland, Oregon, June 2005.
19. E. Tatlicioglu D. Dawson , M. McIntyre, and I. Walker, "Adaptive Nonlinear Tracking Control of Kinematically Redundant Robot Manipulators with Sub-Task Extensions," *Proceedings of the 2005 IEEE Conference on Decision and Control*, Seville, Spain, 2005, To be submitted.
20. N. Bernstein, *The Coordination and Regulation of Movement*, Pergomon Press, London, 1967.
21. B. Tuller, M.T. Turvey, and H.L. Fitch, "The Bernstein perspective: II. The concept of muscle linkage or coordinative structure," In J. A. S. Kelso (ed.) *Human Motor Behavior: An Introduction*, Erlbaum, NJ, 1982.

*billkier@bio.unc.edu: phone (919) 962-5017; fax (919) 962-1625